N. George, P. Ripka and V. Grim, "C-Shape Busbar With Frequency Invariant Points for Wideband Current Measurement," in IEEE Transactions on Industrial Electronics, vol. 71, no. 6, pp. 6446-6456, June 2024, doi: 10.1109/TIE.2023.3299010.

C-Shape Busbar with Frequency Invariant Points for Wideband Current Measurement

Noby George, Pavel Ripka, *Member IEEE,* and Václav Grim, Student *Member IEEE*

***Abstract*— A yokeless busbar current transducer with frequency-invariant points is presented for the first time in this paper. Existing rectangular busbar current transducers suffer from the frequency dependency issue due to the eddy currents in the massive busbar. The proposed transducer has a novel C-shaped structure for the sensing area of the busbar. It is observed for the first time that this structure provides sets of frequency-invariant points on both sides of the C- shaped busbar. In the proposed scheme, two integrated fluxgate sensors in differential form are used to measure the magnetic flux densities at those invariant points. A Finite Element Method (FEM)-based 3-D analysis performed using the Ansys Maxwell eddy current solver provided the exact locations of the frequency-invariant points. A prototype was made, and functionality tests of the C-shape busbar transducer have been carried out in the laboratory using DRV-425 integrated fluxgate sensors from Texas Instruments. In the experiment, fluxgate sensors placed at frequency-invariant points measured the flux densities at multiple frequencies varying from 50 Hz to 1000 Hz. The results obtained from the tests showed that the error due to frequency dependency has been reduced from 14 % to 0.85 % using the proposed C-shape busbar.**

***Index Terms*—Current measurement, Fluxgate sensor, Busbar, Frequency-invariant point, Eddy currents.**

I. Introduction

Accurate current measurement for a wide frequency range is vital in various power electronic and industrial applications [1]-[3]. Magnetic field sensor-based yokeless current transducers [4]-[6] are lightweight. In addition, they do not have core saturation issues, they have a bandwidth range from DC to kHz, which can be increased up to MHz [7]. Yokeless current transducers are used for measuring the current in massive rectangular busbar conductors [8]. In yokeless busbar current transducers, the magnetic field sensors are placed outside the busbar in circular [8]- [9], differential [10], and elliptical array [11] form to sense the magnetic flux density that is proportional to the current in the busbar. The magnitude of the flux density outside the rectangular busbar is dependent on the frequency of the current in the busbar due to the eddy current effect and the asymmetric shape of the busbar [12] – [13]. It is important to pay attention to this frequency dependency for wideband current measurement in rectangular busbar because it limits the bandwidth of the transducers even if the bandwidth of the magnetic field sensor used in the yokeless transducer is wide enough.

A small number of published papers [12]- [15] mention about the frequency dependency in yokeless busbar current transducers and suggest compensation techniques. A digital filter-based frequency compensation approach for yokeless busbar current transducer is presented in [12]. It uses an array of 8 Hall-Effect sensors around the busbar, and it relies on simulation studies to position the sensors around the conductor and design suitable filters for each of the sensors. This is a complex procedure, because the frequency characteristics at each of the sensor points are different. In addition, exact positioning of the magnetic field sensors around the bus bar is difficult. A TMR-based transducer with an optimization algorithm to position the sensors around a 20×3mm busbar is presented in [13]. The current density distribution studies at DC and 50 Hz used for position optimization show that the eddy current effect is not properly taken into consideration [13].

Differential arrangement-based yokeless current transducers are lightweight, easy to install, require less access to the busbar conductor, and partially cancel the effect of an external homogeneous magnetic field [16]. Existing differential busbar current transducers use a cylindrical hole in the bus bar to position the fluxgate sensors [14], [15]. The frequency error of the basic setup is 14 % at 1 kHz. An amphitheatre structure for the busbar [14] with a cylindrical hole reduced the frequency error to 9 %, while a non-uniform structure [15] for the busbar helped to reduce the frequency error to ±3 % at 1 kHz. The disadvantage of these techniques is that they need a hole in the middle of the busbar to place the sensors, and any geometry mismatches in the structure lead to errors in the measurement.

A fluxgate magnetic sensor-based differential busbar current transducer with frequency-invariant sensing points is presented in this paper. A simple and novel C-shape structure for the busbar helps to obtain two frequency-invariant points on both sides of the C-shape part of the busbar. The point is called frequency-invariant because the magnitude of the flux density

Noby George, Pavel Ripka, and Václav Grim are with the Faculty of Electrical Engineering, Czech Technical University, Prague, Czech Republic (e-mail: noby.george@fel.cvut.cz, ripka@fel.cvut.cz, and vaclav.grim@fel.cvut.cz,).

at this point does not vary with the frequency of the busbar current. The novelties and advantages of the proposed transducer compared to the existing frequency compensation techniques are summarized and given below.

- We present in this paper for the first time that a simple C-shape structure for the busbar helps to obtain frequency-invariant points in the C-shape sensing part of the busbar.
- The frequency-invariant points exist like pairs on both sides of the C-shape sensing part, and it helps for the differential placement of magnetic field sensors at the invariant points.
- The proposed C-shape structure for the busbar reduces the frequency dependency to 0.85 % at 1 kHz. This is much better than the frequency compensation techniques based on amphitheatre (9% error at 1 kHz) [14] and wedge shape structures (±3% error at 1 kHz) [15] for the busbar. Also, the proposed technique does not require complex digital filtering (1.2 % at 2.5 kHz) [12] or position optimization algorithms (1.5 % at 1 kHz) [13].
- The frequency-invariant points help to compensate for the frequency dependency for higher frequencies also (more than 1 kHz).
- The proposed C-shape structure not only provides one pair of basic frequency-invariant points but also multiple frequency-invariant points on both sides of the C-shape busbar. It enables reliable placement of micro-fluxgate sensors in differential form and measure wider range of current.

The article is organized as follows. Details about the C-shape structure of the busbar and the frequency-invariant points are provided in section II. An experimental analysis and a 3D FEM-based detailed analysis of the proposed current transducer are presented in section III. A comparison of features and a discussion about the proposed C-shape busbar is provided in section IV. Section V provides the conclusions.

II. The C-Shape Busbar Current Transducer with Frequency-Invariant Points

Details of the proposed frequency-independent C-shaped busbar and the differential arrangement of the fluxgate sensors at the frequency-invariant points are presented in this section of the paper.

A. The C-Shape Busbar and the Frequency-Invariant Point

Earlier studies have shown that the frequency dependency of the yokeless current transducer for a rectangular busbar can be improved by a suitable geometrical modification to the busbar [14], [15]. The authors have conducted a series of FEM-3D analyses in this direction, by trying different geometric modifications to the busbar. The aim behind the analysis was to get sensing points/locations for the transducer in which the magnitude of the flux density (*B*) at these points should be minimally affected by the frequency of the busbar current. The magnitude of the flux density at any point around a long rectangular conductor can be obtained from Ampere's circuital law, as in (1).

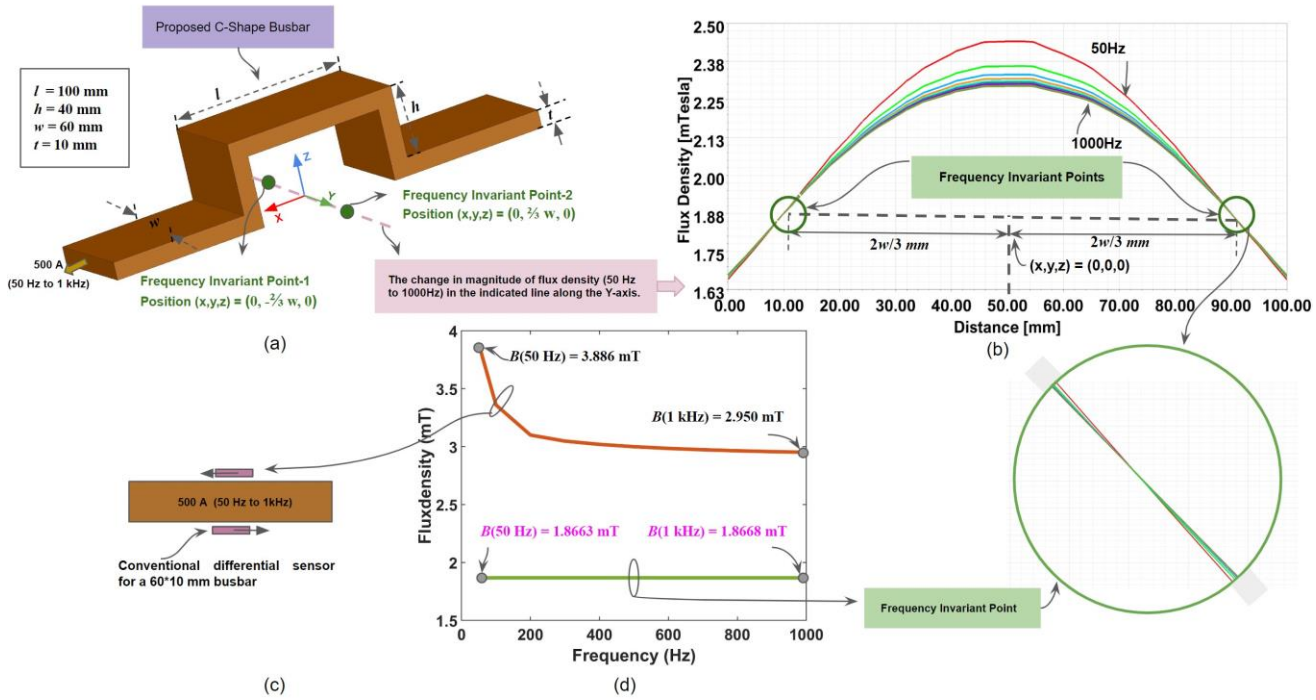

Fig. 1. (a) The dimensions of the proposed C-shape busbar and the locations of the two basic frequency-invariant point (b). In the case of a conventional differential busbar current transducer, the magnitude of the flux density at the sensor locations varies with the frequency (c, d). The 3D-FEM results show that the frequency-invariant point helps to obtain an almost constant magnitude of the flux density for a wide frequency range (d).

$$\oint B.dl = \mu_0 I \quad (1)$$

In (1), I is the total current enclosed in the closed integral path, and it does not vary with the frequency. Due to the eddy current in the busbar, B at a given point in the case of a long rectangular busbar changes with frequency [12]-[15]. It is observed from FEM analysis that for some locations B increases with frequency, while for other locations B decreases with frequency. This led us to think that there may be a point at which magnitude of B is independent of the frequency of the current. Although we could not find a frequency-invariant point in the vicinity of a long rectangular bus bar, we were able to find such points if we used a C-shaped structure for the busbar in the measurement location. The frequency-invariant points found during the 3D-FEM analysis of a C-shape structure for the busbar are shown in Fig. 1a and b.

The dimensions of the proposed C-shape busbar are shown in Fig. 1a. The total height (h+t) of the C-shape part is half of its length (l). During the FEM analysis using the Ansys Maxwell eddy current simulator, a current of 500 A is passed through the C-shape bus bar and the frequency is varied from 50 Hz to 1000 Hz. The variation of the magnitude of the resultant flux density through a line passing through the center of the C-shape, along the Y-axis (for X and Z = 0), is shown in Fig. 1b. The Ansys Maxwell Eddy current solver provides the magnitude of the resultant of flux density (in the X, Y, and Z direction) for each point in the line through the Y-axis. Fig. 1b shows two basic frequency-invariant points at a distance 2w/3 from the origin, which is 1 cm from the edge of the busbar on both sides.

B.The Differential Busbar Current Transducer

The differential current transducer arrangement requires two magnetic field sensing elements on both sides of the conductor or busbar, as shown in Fig. 1c. A conventional differential busbar current transducer is frequency-dependent, as shown in Fig. 1.d. The two basic frequency-invariant points on both sides of the proposed C-shape busbar help to form a differential current transducer that can perform frequency-independent current measurements. The magnitude of B at frequency invariant for a 500 A current in the busbar is 1.88 mT (as shown in Fig. 1d). So, the C-shape busbar helps to use the highly precise and linear fluxgate sensor to form the differential current transducer (as shown in Fig. 2a). The sensing range of commercially-available fluxgate sensor DRV-425 is ±2mT [17]. Fluxgate sensors S1 and S2 have been placed at the frequency-invariant points in such a way that their axis of sensitivity is aligned with the resultant flux density vector at that point (as shown in Fig. 2c). The output voltages V_{s1} and V_{s2} of the fluxgate sensors are given to a summing amplifier to cancel the effect of the external homogeneous magnetic field, and to get an average of both V_{s1} and V_{s2}. The frequency dependency of the output voltages of the fluxgate sensors (V_{s1} or V_{s2}) and the summing amplifier (V_{out}) is analyzed and presented in the next section of the paper.

III. Experimental and 3D FEM-Based Analysis of the Proposed Transducer

The FEM-based analysis of the proposed C-shape busbar wideband current transducer is performed using a 3D model of the busbar in the Anysys Maxwell Eddy current solver. The details about the analysis parameters used in the 3D-FEM model are provided in Table I. The experimental analysis of the wideband busbar transducer was done with the help of suitable prototypes of the C-shape busbar and differential transducers developed in the laboratory.

A. The Prototype of the C-shape Busbar-Based Wideband Differential Current Transducer

A suitable prototype of the proposed copper C-shape busbar (dimensions given in Fig. 1a) is developed in the laboratory and tested. A picture of the prototype of the busbar is given in Fig. 3a. A suitable prototype for a differential current transducer is developed using the fully-featured evaluation modules of integrated fluxgate sensors DRV-425 from Texas Instruments [18]. The fluxgate sensor DRV-425 is specially designed for

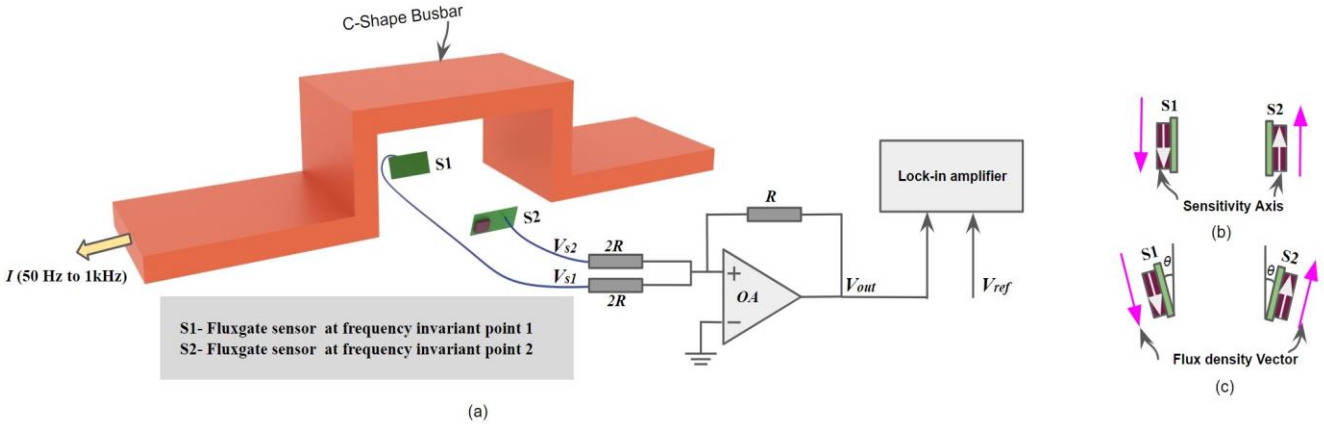

Fig. 2. (a) A schematic representation showing the fluxgate sensors kept in differential form at the basic frequency-invariant points. A suitable sensor holder is used in the laboratory to position the sensors. It is not shown in this figure for easy viewing of the sensor locations. (b) The axis of sensitivity of the sensor is aligned with the tangential component of the flux density at the frequency-invariant point by adjusting angle θ (c).

TABLE I
FEM (3D) SIMULATION PARAMETERS

Software & Properties	Description	Notes
Software	Ansys Maxwell	
Solver	Eddy Current	
Busbar material	Solid Copper	Default material settings with relative permeability 0.99991
Boundary Condition	Natural (between objects) & Neumann boundaries (for exterior boundary)	Default boundary for Ansys Maxwell 3D solver
Mesh type	Adaptive Mesh Refinement	Length element-based refinement with 100000 additional elements
Analysis set-up	Number of passes = 100, Percent error = 0.5 %, Adaptive Frequency = 1000 Hz, Frequency sweep = 50 Hz to 1000 Hz	

busbar current-sensing applications [19]. It has a bandwidth of 47 kHz, linearity ±0.1 %, ±5 nT/°C offset drift with temperature, and noise of 1.5 nT/√Hz. The fluxgate sensors are positioned in the frequency-invariant points using a suitable non-magnetic 3D-printed holder developed in the laboratory. The holder allows X, Y, and Z axis movement of the fluxgate sensors, as marked in Fig. 3b. The holder helps to accurately position the sensors in the frequency-invariant point and also to check the frequency characteristics near the frequency-invariant points. A picture of the fluxgate sensors positioned at the frequency-invariant point is shown in Fig. 3c. The summing amplifier is developed using a low-noise (2.8 nV/√Hz) and precise Operational Amplifier (OA) ADA4075 from Analog Devices.

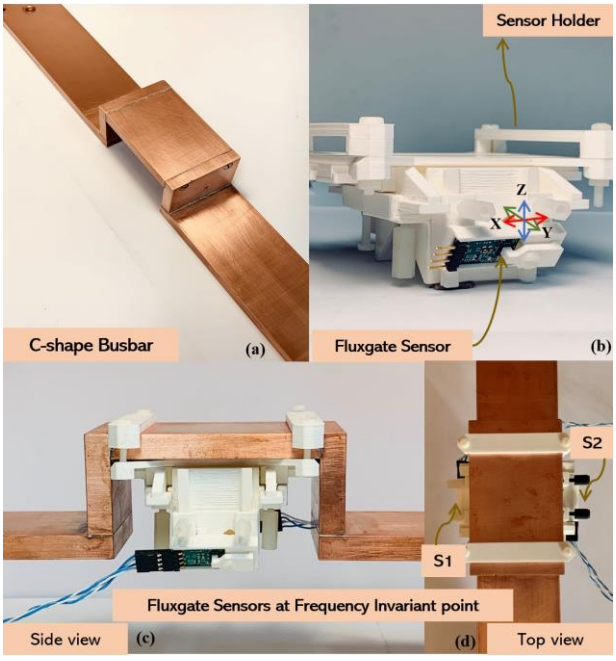

Fig. 3. (a) The prototypes of (c) the C-shape busbar, and (b) the sensor holder. The fluxgate sensors kept at the frequency-invariant point shown in (c), and (d).

B. The Measurement Setup

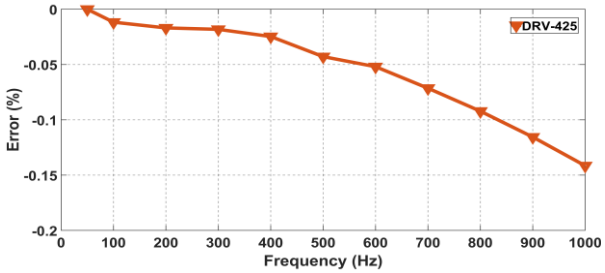

Fig. 5. The frequency-dependent error characteristics of the fluxgate sensor DRV-425.

Fig. 4. The block diagram representation of the measurement system developed in the laboratory.

A measurement system that can analyze the frequency characteristics of the proposed current sensor has been developed in the laboratory. The block diagram representation of the developed measurement system is provided in Fig. 4. The AC current with constant amplitude and frequency range from 50 Hz to 1000 Hz is passed through the proposed C-shape busbar using the arbitrary waveform generator 3390 from Keithley and power amplifier 7548 from AE Techron Inc. The frequency characteristics of the output voltages (V_{s1} and V_{s2}) of the fluxgate sensors and of the summing amplifier (V_{out}) are analyzed using the SRS-830 lock-in amplifier from Stanford Research Systems. The input noise of SRS-830 is 6 nV/√Hz at 1 kHz. The reference (V_{ref}) to the Lock-in amplifier is provided from a 4-terminal power-current-sensing foil resistor VCS-301 from Vishay Precision Group.

C. Frequency Characteristics of the C-shape Busbar Based Wideband Differential Current Transducer

The frequency characteristics of the DRV-425 integrated fluxgate sensor is tested in the laboratory before they are used to measure the flux density values at the frequency-invariant points. A single DRV-425 fluxgate sensor is kept close to a circular conductor and the frequency is varied from 50 Hz to 1 kHz for constant current. The characteristics obtained are shown in Fig. 5. It is clear from Fig. 5. that the DRV-425 fluxgate magnetic field sensor is capable of measuring flux density up to 1kHz with 0.15 % frequency error.

The functionality of the proposed current transducer is tested with the help of 3D-FEM analysis and using the suitable wideband transducer (as shown in Fig. 3) developed in the laboratory. The fluxgate sensors are kept at the basic frequency-invariant points, and the frequency characteristics of each of the fluxgate sensors (V_{s1} and V_{s1}) and the summing amplifier (V_{out}) are obtained. The individual fluxgate sensors (in differential form), and the summing amplifier output showed similar frequency characteristics. The obtained characteristics are provided in Fig. 6. The relative error at each frequency (f) is calculated using (2). The V_{out} in (2) changes to V_{s1} and V_{s2} for analyzing the frequency characteristics of individual sensors S1 and S2.

$$Error\ (\%) = \frac{V_{out\,(50Hz)} - V_{out\,(f)}}{V_{out\,(50Hz)}} \times 100 \qquad (2)$$

The result presented in Fig. 6 shows the frequency dependancy of the C-shape busbar transducer at the basic frequency invariat point. The 3D-FEM result shows idealy flat characterstics confirming the magnitude of flux density at the frequency invariant point is not changing with frequency. A 500 A and 15 A current excitation is used in the 3D-FEM analysis and the same charactertics as shown in Fig. 6 is obtained in both the cases. A constant 15 A current is passed through the prototype of the C-shape busbar (keeping fluxgate sensors at

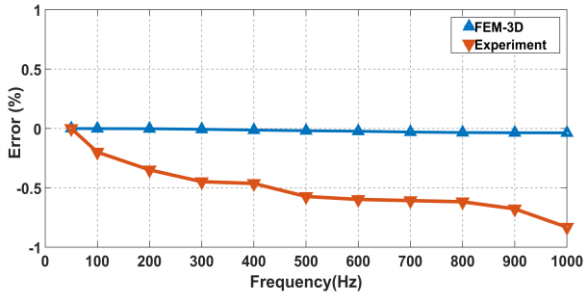

Fig. 6. The frequency-dependent error characteristics of the proposed current transducer at the basic frequency-invariant point.

frequency invariant point) and the frequency characteristics (for 50 Hz to 1000 Hz) are provided in Fig. 6 along with the 3D-FEM results. The 15 A is the maximum current obtained at 1000 Hz from the power amplifer using the measurement set up provided in Fig. 4. The maximum % error noted in the experimental analysis is – 0.85 % at 1 kHz. We believe that the error is caused by mechanical tolerances, also we verified that the error is not caused by conductive objects in the vicinity. The phase difference between the proposed transducer output and the current sense resistor output is obtained using the lock-in amplifier and is provided in Fig. 7.

D. Frequency Characteristics of the Transducer in the Vicinity of the Basic Frequency-Invariant Points

The frequency dependancy of the of the C-shape busbar transducer at the points near to the frequency invariant points in X, Y and Z directioins are analysed in this section. To do this analysis, initially, the positions of sensors S1 and S2 were moved (using the holder) along the Y-axis by 10 mm (X and Z displacement = 0) in both directions from the frequency-

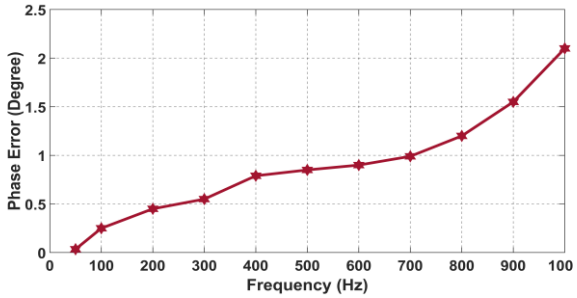

Fig. 7. The phase error of the proposed wideband differential current transducer.

invariant points (The X, Y, and Z directions are marked in Fig. 1). The relative % error at each position is obtained by comparing the voltage output (V_{out}) at 50 Hz and at 1 kHz, using (2). The results are presented in Fig. 8. After the Y-axis displacement analysis, the Y-axis position of sensors S1 and S2 is kept fixed at the frequency-invariant point (*2w/3*), and the sensors are moved through different locations along the X-axis (Z displacement = 0). The characteristics of the transducer if it moves from the frequency invariant point in the X-direction are presented in Fig. 9. The Z-axis displacement also showed similar results to the X-axis displacement characteristics. It is clear from Figs. 9 and 10 that any movement of fluxgate sensors S1 and S2 from the frequency-invariant point is prone to introduce error into the measurement. The frequeny depdenacy at 10 mm from invariant point in Y-direction is -2.5%, while a 20 mm displacement from basic invariantg point

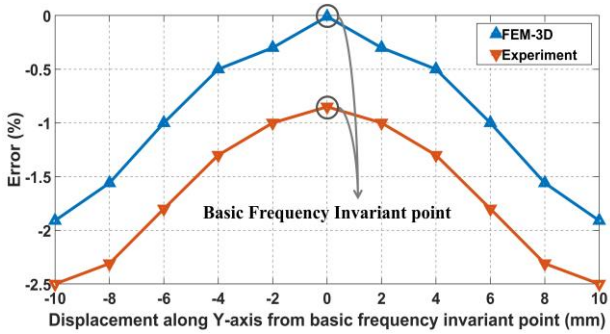

Fig. 8. The frequency error characteristics of the wideband transducer when the sensors move away from basic invariant points in the Y-direction.

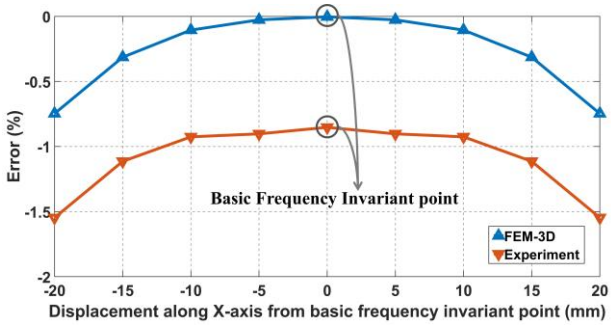

Fig. 9. The frequency error characteristics of the wideband transducer when the sensors move away from the basic invariant points in the X-direction.

in X or Z direction cause -1.58 % of frequency dependancy. This also shows the importance of a frequency-invariant point.

E. Presence of Multiple Frequency-Invariant Points in the C-Shape Part of the Busbar

The analysis of Fig. 9 showed that the displacement of the fluxgate sensors from the invariant point in the X-axis direction has less effect (less than 1% error for 10mm displacement). We found this interesting, and we checked the reason behind it by conducting 3D-FEM and experimental studies. The studies showed that there are multiple frequency-invariant points in the C-shape part of the busbar. As mentioned earlier, the center basic frequency-invariant points exist in a line through the Y-axis for X and Z distances equal to zero. To find other invariant points using 3D-FEM, different lines are drawn along the Y-axis (i) for different X-positions (keeping Z= 0), and (ii) for different Z-position (keeping X= 0). A schematic representation of the same is provided in Fig. 10. In Fig. 10, *Xd*, *Yd*, and *Zd* denote the distance of the new invariant from the basic invariant point in the X, Y, and Z directions. The locations of the multiple frequency invariant points obtained from FEM studies is verified using the experimental studies conducted in the laboratory and it is provided in Fig. 11 and 12. The multiple frequency invariant points in the vicinity of basic frequency invariant point-2 are shown in Fig. 12, and Fig. 13. A similar set of invariant points exist near basic invariant point-1 also, with same *Xd*, *Yd* and *Zd* distances. So, all the frequency invariant points found exist like pairs (as shown in Fig. 1b.) on both sides of the busbar so that the differential measurement of current is possible. All the multiple frequency invariant points obtained showed frequency characteristics like the basic invariant points (as in Fig. 6).

It is interesting to notice from Fig. 12. that the frequency invariant points in the negative Z- direction move away (indicated as positive Y_d) from the edge of the C-shape part of the busbar. The magnitude of the flux density at the invariant points that are away from the busbar is analyzed and presented in Fig. 13. The current through the busbar during the 3D-FEM

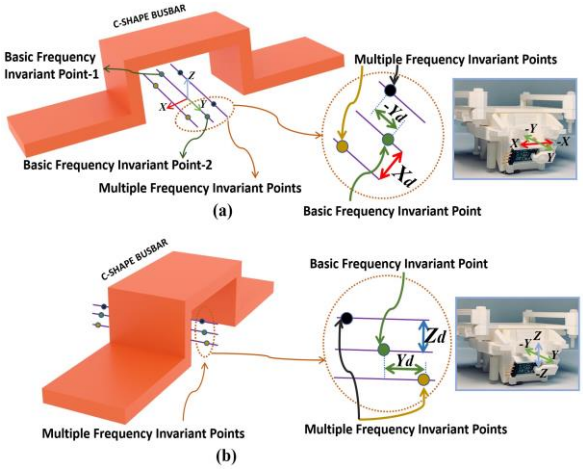

Fig. 10. The schematic representation of multiple frequency invariant points along Y-axis for different (a) X-axis, and (b) Z-axis positions. The sensor holder indicating sensor movement direction is shown. This holder is developed to conduct the study. In practice, the sensor position can be fixed.

analysis was 1 kA. It is visible from Fig. 13 that the magnitude

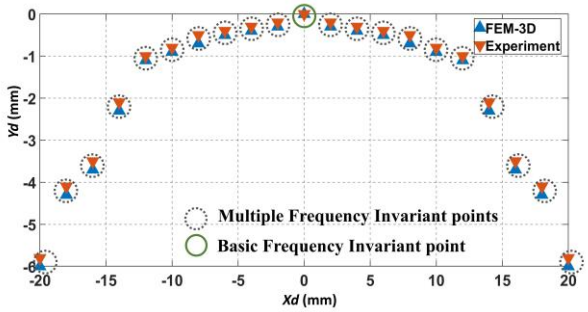

Fig. 11. The various frequency-invariant points obtained at different locations along the Y-axis for different X-positions (keeping Z= 0, according to Fig. 10a).

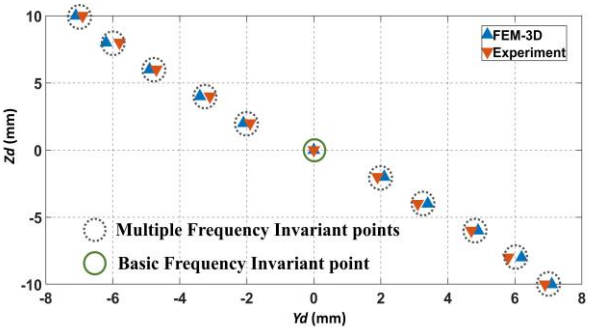

Fig. 12. The various frequency-invariant points obtained at different locations along the Y-axis for different Z-positions (keeping X= 0 according to Fig. 10b).

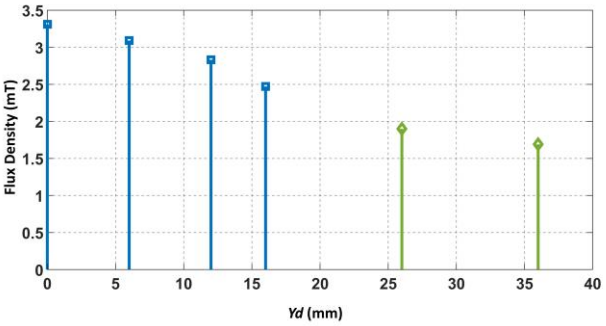

Fig. 13. The magnitude of the flux density at the multiple frequency-invariant points along the Y-axis, for different Z-positions for 1 kA current (keeping X= 0, according to Fig. 10b). The fluxgate sensors can be positioned at the invariant points where flux density is below 2 mT. This is an advantage of having multiple frequency-invariant points.

of flux density is below 2 mT at the frequency invariant points that are at a distance *Yd* = 26 mm (*Zd* = -40mm) or more. This helps to measure higher currents, independent of frequency, using the same C-shape structure and fluxgate sensors DRV-425.

F. The Experimental Analysis Of The Transducer at High Current And Frequency Ranges

The analysis presented in the previous section shows the existence of the multiple frequency invariant points and their importance in extending the current measurement capability of the proposed transducer. To verify this experimentally, the measurement setup is modified to pass current up to 1 kA through the C-shape busbar. A block diagram representation of

the new measurement setup is provided in Fig. 14. The output of the AE Techron 7548 power amplifier is connected to the secondary side of a 2000 VA, 50 Hz Current Transformer (CT), and the primary side is shorted through the C-shape busbar using proper cables. This provides up to 1 kA at 50 Hz. During the analysis, the magnitude of the current through the C-shape busbar is varied from 0 to 1 kA and the fluxgate sensors were kept at an invariant point that is at a distance of Yd = 38 mm and Zd = -40 mm (as shown in Fig. 10, and Fig. 13) from the basic invariant point. The actual current is measured using the LEM IT-1000S current sensor with a measurement range of up to 1 kA and an accuracy of 0.0054 %. The change in output voltage (V_{out}) of the proposed transducer with a change in current through the C-shape busbar is provided in Fig. 15. It is visible from Fig.15 that the proposed wideband C-shape busbar transducer with multiple frequency invariant points can measure current up to 1 kA. Also, the experimental results verify that the magnitude of the flux density at this frequency invariant point is below 2 mT. The output from the proposed wideband transducer is highly linear and the maximum linearity error noted is -0.33 % of full-scale. The fluxgate sensors in differential form were also kept at the basic invariant points and they measured up to 500 A with a similar linear output shown in Fig.15. Along with analyzing the capability to measure 50 Hz current the ability of the proposed transducer to measure the high-frequency current is also experimentally verified in the laboratory. The current through the C-shape wideband busbar is varied from 0 to 90 A (maximum current provided by the set-up at 1 kHz) at 1000 Hz and the corresponding change output of the proposed transducer is provided in Fig. 16. The Fig. 16 indicates that the transducer provides linear output for high-frequency current.

The frequency dependency of the proposed wideband transducer is tested up to 1 kHz range in the previous sections to compare its performance with other compensation techniques [12]- [15] with similar ranges. The frequency invariant point presented in this paper holds its property for higher frequencies also. The 3D-FEM analysis showed very less (similar to Fig. 6) frequency dependency up to 3.5 kHz. The magnitude of the flux density at the invariant point remains same for frequency up to 3.5 kHz in the FEM analysis. The frequency dependency of the proposed C-shape busbar is tested in the laboratory up to 3.5 kHz using the measurement set-up provided in Fig. 14. The current in the C-shape busbar was kept constant at 20 A and the

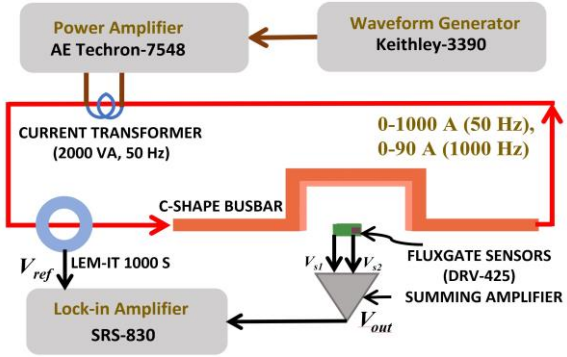

Fig. 14. The block diagram representation of the set-up developed in the laboratory to pass high current through the C-shape busbar.

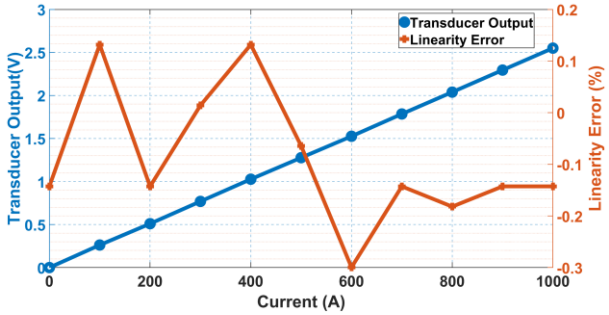

Fig. 15. The output of the proposed transducer at 50 Hz current up to 1 kA. It shows the ability of transducer to measure wide range of current.

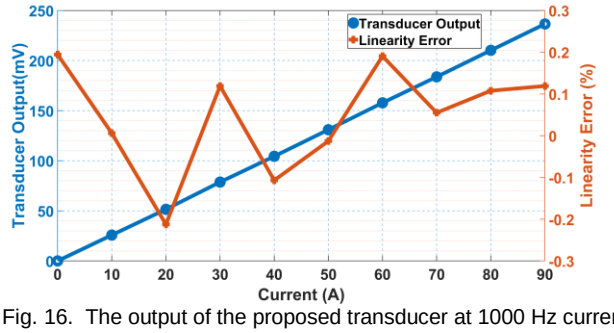

Fig. 16. The output of the proposed transducer at 1000 Hz current.

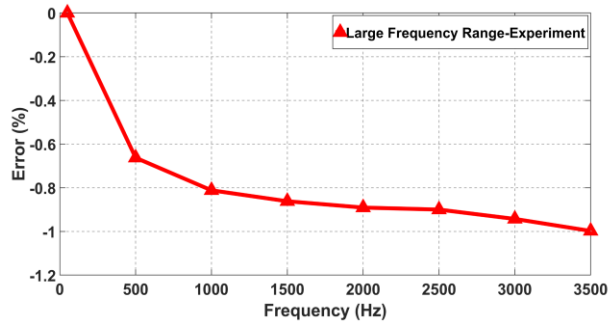

Fig. 17. The frequency dependancy of the proposed transducer for high frequency range.

frequency is varied from 50 Hz to 3.5 kHz. The results are presented in Fig. 17. The maximum error noted in the analysis is 0.998 % at 3.5 kHz.

G. The Effect of a Nearby Rectangular Busbar on the Proposed Wideband Differential Current Transducer

The effect of a nearby external rectangular current-carrying busbar on the performance of a C-shape busbar differential current transducer is presented in this section. The C-shape busbar and the external rectangular busbar (60 mm×10 mm) carry constant current with frequencies from 50 Hz to 1000 Hz. The study (both the busbars were rectangular) presented in [16] shows that the effect of the external field depends on the angular position of the nearby busbar. In this study, the external busbar is kept at distance of 125 mm from the C-shape busbar at different vertical positions, as shown in Fig. 18. The studies conducted in this direction showed that the effect of the external busbar is less on the basic frequency invariant points when the rectangular busbar is kept at a vertical height equal to half of the total height (h+t) of the C-shape part of the busbar. The

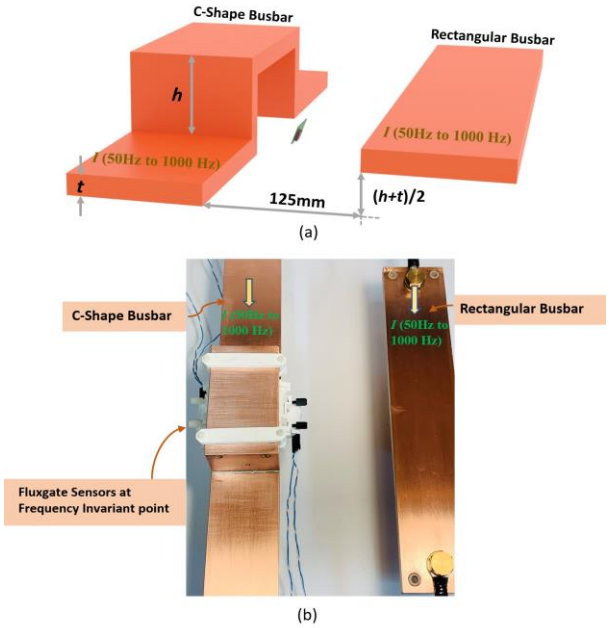

Fig. 18. (a) Schematic and (b) Experimental photographs showing the test condition for a nearby rectangular busbar conductor.

maximum relative error noted is 1.52 % at 1 kHz, and the same is provided in Fig. 19.

IV. Discussion

The comparison of the main features of the proposed transducer with existing techniques, applications, and scope for future work is discussed in this section.

A. Compariosn of Features

The features of the proposed C-shape busbar wideband current transducer are compared with the existing frequency

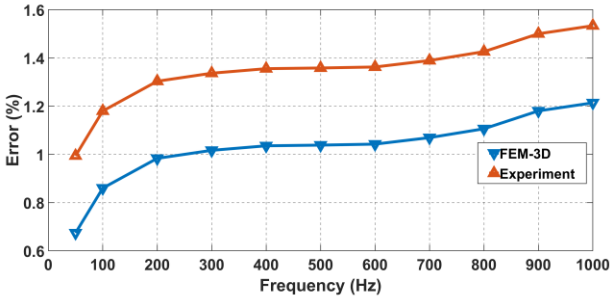

Fig. 19. The frequency characteristics of the frequency-invariant point with the rectangular busbar interference.

compensation technique used to increase the bandwidth of rectangular busbar current transducers, and are provided in Table II. The existing techniques include geometrical modifications for the busbar [14], [15], digital compensation based on an arbitrary magnitude filter and a 20-order frequency compensation filter [12], also adjusting the position of the sensors relative to the busbar using optimization algorithms [13]. The frequency-invariant points are not presented in any of the frequency compensation methods. The sensitivity of the proposed transducer is 2.5 mV/A for 1 kA current and 1 kHz frequency ranges. The multiple invariant points present in the C-shape transducer helps to increase the current measurement range to 1 kA at 50 Hz, which is much better compared to the digital filter (200 A, uses Hall-Effect sensors) [12] and position optimization (600 A, uses TMR sensors) [13] based approaches. The frequency range of the proposed wideband transducer is not limited to 1 kHz. The experimental analysis showed 0.998 % error at 3.5 kHz and extending range beyond 1 kHz does not require any design changes in the proposed transducer, unlike other compensation schemes [12]- [15]. The proposed transducer also maintains a competitive size and cost. In addition, the new method presented in this paper is simple by design and complexity in manufacturing the shape is less compared to the other geometrical modification-based

TABLE II
COMPARISON OF FEATURES

Compensation Technique	Uses C-Shape Busbar	Frequency invariant point present	Type & Number of Magnetic Field (MF) Sensors	Size & Complexity	Cost	Current Range	Frequency Range	Maximum % Error
Amphitheater Busbar Structure [14]	No	No	Fluxgate -2	Medium	Low	1000 A	1 kHz	9%
Wedge Shape Busbar Structure [15]	No	No	Fluxgate-2	Medium	Low	1000 A	1 kHz	±3%
Digital Filter [12]	No	No	Hall-Effect-8	Large	High	200 A	2.5 kHz	1.2%
Position Optimization Algorithm [13]	No	No	TMR -4	Medium	High	600 A	1 kHz	1.5%
This Paper	Yes	Yes	Fluxgate-2	Medium	Low	1000 A	1 kHz *	0.85%

*= The frequency range is not limited to 1 kHz (0.998% error at 3.5 kHz).

frequency compensation approaches [14]- [15]. A suitable sensor holder which can move in all the X, Y, and Z directions has been developed in the laboratory for experimental verification of the multiple frequency-invariant points. A simple holder can be used to position/hold the magnetic field sensor in the frequency-invariant points in differential form and measure the current.

B. Applications and Scope for Futurework

The coreless busbar current transducers available in the market [20]- [21] use either fluxgate or Hall-effect sensors in differential form for the measurement of current in busbar for Electric Vehicles and power electronic drives. The effect of eddy current in rectangular busbar affects the performance of such transducers and it is addressed in this manuscript. So, the proposed C-shape busbar-based transducer is well applicable and efficient for the measurement of current in Battery Management Systems (BMS) of Electric Vehicles (EVs), motor drives, and solar inverters.

The proposed C-shape busbar wideband transducer presented in this paper showed -0.85 % frequency dependency at 1 kHz and -0.998 % at 3.5 kHz. We plan to enhance the frequency dependency of the transducer developed in the laboratory in the future by analyzing the effect of mechanical tolerance and inductance of the C-shape busbar, which is found as 232.762 nH at 50 Hz and 226.735 nH at 1000 Hz using the 3D-FEM model.

V. Conclusion

A novel wideband yokeless differential busbar transducer based on frequency-invariant points is presented in this paper. We show in this paper for the first that a simple C-shape structure for the busbar provides frequency-invariant points at which the magnitude of the flux density does not vary with the frequency of the current in the busbar. The frequency-invariant points exist on both sides of the C-shape part of the busbar as pairs so that a differential current measurement is possible. The experimental studies conducted on the prototype developed in the laboratory showed -0.85 % frequency dependency at 1 kHz, which is better compared to other frequency compensation techniques available for the 1 kHz range [12]- [15]. The main advantages of the proposed transducer also include (i) it is easy to manufacture (also without affecting the current carrying capacity of the busbar) compared to other geometry modification-based compensation [14]- [15] (ii) it does not require digital filters or sensor position optimization algorithms that are otherwise required for wideband current measurement in rectangular busbar [12]- [13] (iii) the frequency range is not limited to 1 kHz (iv) the C-shape structure for busbar provides the possibility to get multiple frequency-invariant points in the C-shape sensing part of the busbar.

References

[1] P. Ripka, "Electric current sensors: A review", *Meas. Sci. Technol.*, vol. 21, no. 11, pp. 1-23, 2010.

[2] S. J. Nibir and B. Parkhideh, "Magnetoresistor with planar magnetic concentrator as wideband contactless current sensor for power electronics applications", *IEEE Trans. Ind. Electron.*, vol. 65, no. 3, pp. 2766-2774, Mar. 2018.

[3] A. Rafiq, S. K. Pramanick and R. Maheshwari, "Design of PCB Coil Based High Bandwidth Current Sensor With Power-Loop Stray Inductance Characterization," *IEEE Trans. Ind. Electron.*, vol. 68, no. 12, pp. 12791-12801, Dec. 2021.

[4] N. George and S. Gopalakrishna, "Development of a new low-cost and reliable core-less current probe for conductor with reduced access", *IEEE Sensors J.*, vol. 17, no. 14, pp. 4619-4627, Jul. 2017.

[5] R. Weiss, R. Makuch, A. Itzke and R. Weigel, "Crosstalk in Circular Arrays of Magnetic Sensors for Current Measurement," *IEEE Trans. Ind. Electron.*, vol. 64, no. 6, pp. 4903-4909, June 2017.

[6] A. Itzke, R. Weiss and R. Weigel, "Influence of the Conductor Position on a Circular Array of Hall Sensors for Current Measurement," *IEEE Trans. Ind. Electron.*, vol. 66, no. 1, pp. 580-585, Jan. 2019.

[7] S. J. Nibir, E. Hurwitz, M. Karami and B. Parkhideh, "A Technique to Enhance the Frequency Bandwidth of Contactless Magnetoresistive Current Sensors," *IEEE Trans. Ind. Electron.*, vol. 63, no. 9, pp. 5682-5686, Sept. 2016.

[8] L. Di Rienzo, R. Bazzocchi and A. Manara, "Circular arrays of magnetic sensors for current measurement", *IEEE Trans. Instrum. Meas.*, vol. 50, no. 5, pp. 1093-1096, Oct. 2001.

[9] R. Weiss, A. Itzke and R. Weigel, "Current measurement of flat conductors with a circular array of magnetic sensors," *2017 IEEE Second International Conference on DC Microgrids (ICDCM)*, pp. 166-170, 2017.

[10] X. P. Xu, T. Z. Liu, M. Zhu and J. G. Wang, "New Small-Volume High-Precision TMR Busbar DC Current Sensor," *IEEE Trans. Magn.*, vol. 56, no. 2, pp. 1-5, Feb. 2020.

[11] R. Weiss, F. Zapf, A. Skelly and R. Weigel, "Busbar Current Measurement With Elliptical Sensor Arrays Without Conductor Specific Calibration," *IEEE Trans. Instrum. Meas.*, vol. 70, pp. 1-9, 2021.

[12] W. Li, G. Zhang, H. Zhong and Y. Geng, "A Wideband Current Transducer Based on an Array of Magnetic Field Sensors for Rectangular Busbar Current Measurement," *IEEE Trans. Instrum. Meas.*, vol. 70, pp. 1-11, 2021.

[13] X. P. Xu, S. Wang, T. Z. Liu, M. Zhu and J. G. Wang, "TMR Busbar Current Sensor With Good Frequency Characteristics," *IEEE Trans. Instrum. Meas.*, vol., vol. 70, pp. 1-9, 2021.

[14] P. Ripka, M. Pribil, V. Petrucha *et al.*, "A Fluxgate Current Sensor With an Amphitheater Busbar," *IEEE Trans. Magn.*, vol. 52, no. 7, Jul, 2016.

[15] P. Ripka, V. Grim, and V. Petrucha, "A Busbar Current Sensor With Frequency Compensation," *IEEE Trans. Magn.*, vol. 53, no. 4, Apr, 2017.

[16] P. Ripka and A. Chirtsov, "Influence of External Current on Yokeless Electric Current Transducers," *IEEE Trans. Magn.*, vol. 53, no. 11, pp. 1-4, Nov. 2017.

[17] "Datasheet for DRV-425," Texas Instruments. [Online]. Available: https://www.ti.com/lit/ds/symlink/drv425.pdf?ts=1665061468436&ref_url=https%253A%252F%252Fwww.ti.com%252Fproduct%252FDRV425.

[18] "DRV425 evaluation module" - Texas Instruments [Online]. Available: https://www.ti.com/lit/ug/slou410b/slou410b.pdf.

[19] "Bus bar theory of operation" - Texas Instruments [Online]. Available: https://www.ti.com/lit/an/sloa237/sloa237.pdf.

[20] "TIPD205 reference design" - Texas Instruments [Online]. Available: https://www.ti.com/lit/ug/tiduaz4a/tiduaz4a.pdf?ts=1681375659315&ref_url=https%253A%252F%252Fwww.google.com%252F

[21] "ACS37610 Coreless Current Sensor" -Allegro Microsystem [Online]. Available : https://www.allegromicro.com/-/media/files/application-notes/an296194-acs37610-busbar.pdf.

Noby George was born in Kannur, Kerala, India. He received the Ph.D. degree in electrical engineering from National Institute of Technology, Rourkela, India in 2019.

He worked as a Research Engineer with the Micelio Mobility Pvt. Ltd, Bengaluru, India, from 2019 to 2021. He is currently working as a Postdoctoral Researcher with Department of Measurement, Faculty of Electrical Engineering, Czech Technical University in Prague. His research interests include development of contactless current and position sensors.

Pavel Ripka (M'2000) was born in Praha, Czech Republic in 1959. He received an Ing. degree in Electrical Engineering in 1984, and CSc. (equivalent to Ph.D.) in 1989. In 1996 he received docent degree.

In 1990 – 94 he was a visiting researcher at the Danish Technical University, in 2001 he was a Marie Curie Advanced Researcher Fellow at University of Galway, Ireland, in 2005/6 he was Visiting scientist at the Institute for the Protection and the Security of the Citizen, Ispra, Italy. Since 2001 he is full professor at CTU, lecturing in Measurements, Engineering Magnetism and Sensors. In 2011-2019 he served as a Dean of Electrical Engineering.

His main research interests are Magnetic Measurements and Magnetic Sensors, especially Fluxgate. He is a co-author of 3 books and 150 journal papers. He also participates in industrial research and holds 12 patents.

Pavel Ripka was Associated Editor of IEEE Sensors Journal, and member of the editorial boards of Technisches Messen, Measurement Science and Technology and Journal of Sensors. He has been a member of the Eurosensors Steering Committee and Program committees of IEEE Intermag and IEEE Sensors conferences. He was a member of ERC panel. He also served as a representative of IEEE Magnetics Society in the IEEE Sensors Council

Full bio can be found at https://measure.fel.cvut.cz/ripka

His lab's webpage is https://maglab.fel.cvut.cz/

Václav Grim (M'18) received the master degree in microelectronics from the National Taiwan University of Science and Technology in 2017 and from the Czech Technical University in Prague in 2018.

He is currently pursuing the PhD degree in electrical engineering at the Department of Measurement, Czech Technical University. His research interests include contactless current and position measurement, material and device characterization, automated test and measurement systems and the design of electronic circuits for sensor data processing.